Understanding ENSO dynamics through the exploration of past climates

Steven J Phipps[1] and Jaclyn N Brown[2]

[1] Climate Change Research Centre, Faculty of Science, University of New South Wales, UNSW Sydney, NSW 2052, Australia
[2] CSIRO Marine and Atmospheric Research, GPO Box 1538, Hobart, TAS 7001, Australia

E-mail: `s.phipps@unsw.edu.au`

Abstract. The palaeoclimate record shows that significant changes in ENSO characteristics took place during the Holocene. Exploring these changes, using both data and models, provides a means of understanding ENSO dynamics. Previous modelling studies have suggested a mechanism whereby changes in the Earth's orbital geometry explain the strengthening of ENSO over the Holocene. Decreasing summer insolation over the Asian landmass resulted in a weakening of the Asian monsoon system. This led to a weakening of the easterly trade winds in the western Pacific, creating conditions more favourable for El Niño development. To explore this hypothesised forcing mechanism, we use a climate system model to conduct a suite of simulations of the climate of the past 8,000 years. In the early Holocene, we find that the Asian summer monsoon system is intensified, resulting in an amplification of the easterly trade winds in the western Pacific. The stronger trade winds represent a barrier to the eastward propagation of westerly wind bursts, therefore inhibiting the onset of El Niño events. The fundamental behaviour of ENSO remains unchanged, with the major change over the Holocene being the influence of the background state of the Pacific on the susceptibility of the ocean to the initiation of El Niño events.

1. Introduction

El Niño-Southern Oscillation (ENSO) is the dominant mode of internal variability within the coupled atmosphere-ocean system, with an irregular period of around two to seven years [1].

The background state of the tropical Pacific Ocean is characterised by a zonal sea surface temperature gradient, with a "warm pool" in the west. These warm surface waters give rise to atmospheric convection, driving easterly trade winds at the surface. These winds advect warm surface waters to the west and cause deeper, colder waters to upwell in the east, therefore maintaining the surface temperature gradient. This gives rise to a background state which is self-reinforcing, but which represents a state of unstable equilibrium. An El Niño event arises when this background state is perturbed. If the easterly trade winds are weakened in some manner, then the warm surface waters in the west flow eastwards. This leads to enhanced sea surface temperatures in the central and eastern Pacific, accompanied by strengthened atmospheric convection and enhanced precipitation.

The palaeoclimate record shows that significant changes in El Niño characteristics have taken place during the past 10,000 years [2–5]. Prior to around 7 ka[1], there was only weak, decadal-

---

[1] ka = thousand years before present

scale variability. "Modern" El Niño activity began around 5–7 ka, with a gradual strengthening of ENSO thereafter. There is evidence of a peak in intensity around 1-2 ka, although strong millennial-scale variability is also apparent [4].

These changes in El Niño have taken place during a relatively quiescent period in the Earth's climatic history, with no significant glaciation or deglaciation. Between 8 ka and the beginning of the pre-industrial era, atmospheric greenhouse gas concentrations were relatively constant, with the CO_2 concentration only varying between 260 and 280 ppm [6]. However, pseudo-cyclic changes in the Earth's orbital geometry have given rise to significant changes in the seasonal cycle of insolation. In particular, at northern mid-latitudes, the amount of insolation during the summer months has decreased by 30–40 Wm^{-2} between 8 ka and the present day.

Modelling studies have shown that the behaviour of ENSO is influenced by the seasonal cycle of insolation in the tropics, and particularly by the amount of insolation during the northern summer [7; 8]. The Asian summer monsoon system has also been shown to play a critical role [9]. However, these studies have used simplified models with a restricted spatial domain [8], or have only considered ENSO behaviour at 6 ka [7; 9].

This study aims to extend the spatial and temporal coverage of previous work by using a global climate model to explore the changes in the climate system over the past 8,000 years. By studying how the forcing "signal" translates into the observed "response", we aim to learn more about ENSO dynamics and, in particular, about the links between ENSO dynamics and global climate change.

2. Modelling experiments

The model used in this study is version 1.1 of the CSIRO Mk3L climate system model, a fully-coupled atmosphere-sea ice-ocean general circulation model [10]. The model comprises atmospheric and oceanic general circulation models, a dynamic-thermodynamic sea ice model and a land surface scheme with static vegetation. The atmosphere model has a horizontal resolution of 5.6°×3.2° and 18 vertical levels, while the ocean model has a horizontal resolution of 2.8°×1.6° and 21 vertical levels.

We conduct equilibrium simulations for 8, 7, 6, 5, 4, 3, 2, 1 and 0 ka. Each experiment differs *only* in that the Earth's orbital geometry is varied; otherwise the model is configured for pre-industrial conditions, with an atmospheric CO_2 concentration of 280 ppm. While this represents a somewhat idealised experimental design, these boundary conditions are nonetheless representative of the true conditions that prevailed during this period. Each simulation is integrated for 1,200 years, with the final 1,000 years being used for analysis.

We find that the model is broadly able to reproduce the trends in ENSO variability over the past 8,000 years (Figure 1). After an initial period of reduced variability, there is a gradual strengthening of ENSO variability after 5 ka, and a peak at 1 ka. Variability in the Niño 3.4 region is 16% weaker at 6 ka than at present. This is consistent with the range of uncertainty within the palaeoclimate record, which indicates a reduction in ENSO variability of 15–60% [11]. We therefore conclude that the model is a useful tool for studying the links between ENSO dynamics and global climate change.

3. ENSO dynamics

We now use the model simulations to follow the physical links within the climate system, as the forcing signal (i.e. the insolation changes) is translated into the observed response. Figure 2a shows the simulated June-July-August surface air temperature at 8 ka, expressed as an anomaly relative to the 0 ka simulation. The increased summer insolation at northern mid-latitudes gives rise to temperatures over land that are up to 4 K higher than at present. However, because the oceans have a much greater heat capacity than the land, the temperature changes over the ocean are smaller.
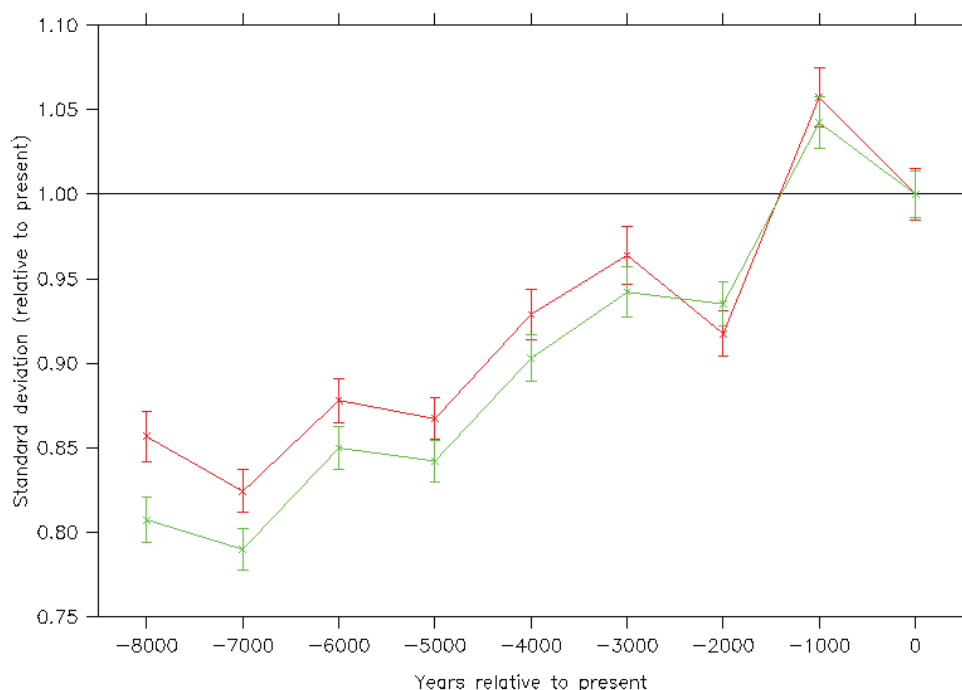
Figure 1. The standard deviation in the simulated monthly sea surface temperature anomalies for the Niño 3 (red) and Niño 3.4 (green) regions, normalised relative to the standard deviation for the present-day simulation. The 95% confidence intervals are shown.

The increased land-sea temperature contrast leads to an intensification of the Asian summer monsoon system, as can be seen in Figure 2b. The mean sea level pressure over the Eurasian and northern African landmasses is reduced by up to 6 hPa, with the enhanced deep convection drawing increased inflows of air from over the tropical Pacific and Indian oceans. The Walker Circulation over the Pacific Ocean is intensified, with an increase in the strength of the easterly trade winds in the central and western Pacific.

The intensification of the Walker Circulation changes the susceptibility of the coupled atmosphere-ocean system to the initiation of El Niño events. Figure 3a shows the propagation of westerly wind bursts within the 0 ka and 8 ka simulations. At 0 ka, most of the wind bursts propagate eastwards to the central Pacific, where they are able to perturb the easterly trade winds and trigger El Niño events. The peak variability in the wind stress occurs at about 160°W. At 8 ka, however, many of the wind bursts are confined to the western Pacific. Peak variability in the wind stresses now occurs at around 160°E, with only a few wind bursts breaking through to the central Pacific. We therefore find that the stronger easterly trade winds act as a barrier, blocking the propagation of westerly wind bursts and inhibiting the onset of El Niño events.

The effects upon ENSO variability are apparent from Figure 3b. At 0 ka, strong, regular El Niño events take place, with peak variability occurring in the central Pacific at around 150°W. At 8 ka, however, El Niño variability is much weaker, consistent with the palaeoclimate record.

The same mechanism is found to operate across all the simulations (not shown). As the summer insolation at northern mid-latitudes decreases from 8 ka to 0 ka, the Asian summer monsoon system and Walker Circulation weaken. The tropical Pacific therefore becomes increasingly susceptible to the initiation of El Niño events. While this mechanism explains the upward trend in ENSO variability over the past 8,000 years, however, it does not account
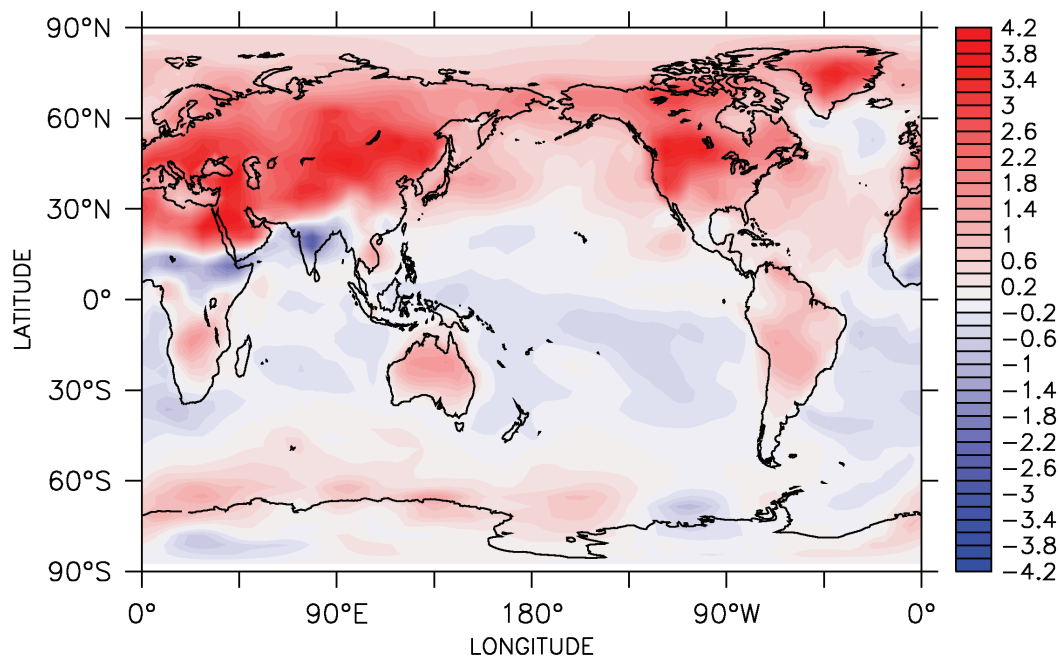
(a) Surface air temperature
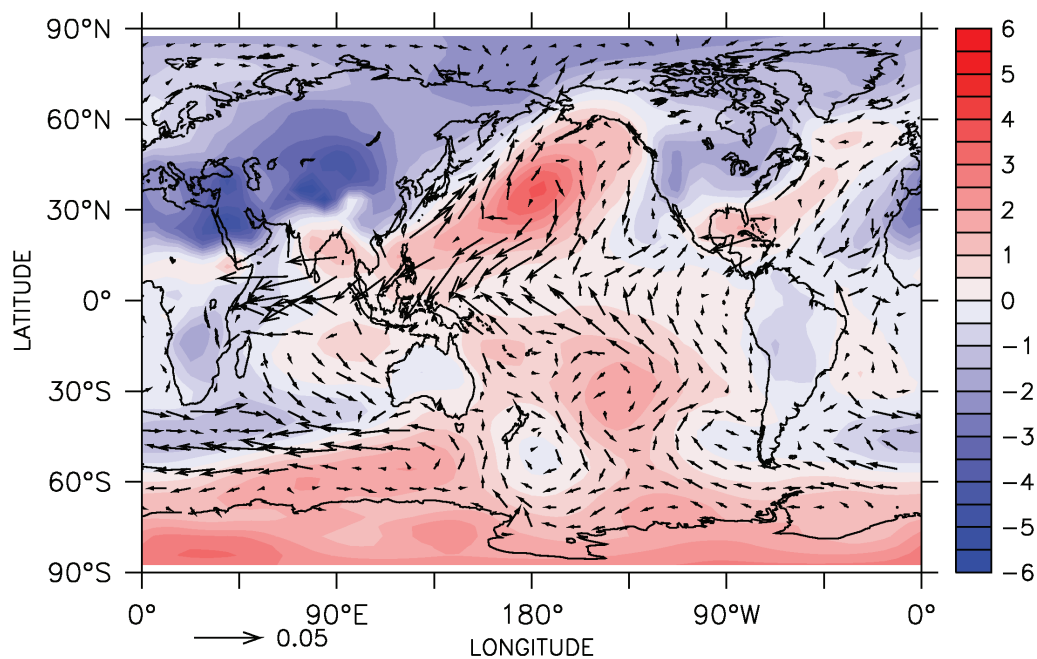
(b) Mean sea level pressure

Figure 2. June-July-August climatologies for the 8 ka simulation, expressed as anomalies relative to 0 ka: (a) surface air temperature (K), and (b) mean sea level pressure (hPa). In (b), the vectors show the surface wind stress anomalies over the ocean (Nm^{-2}).
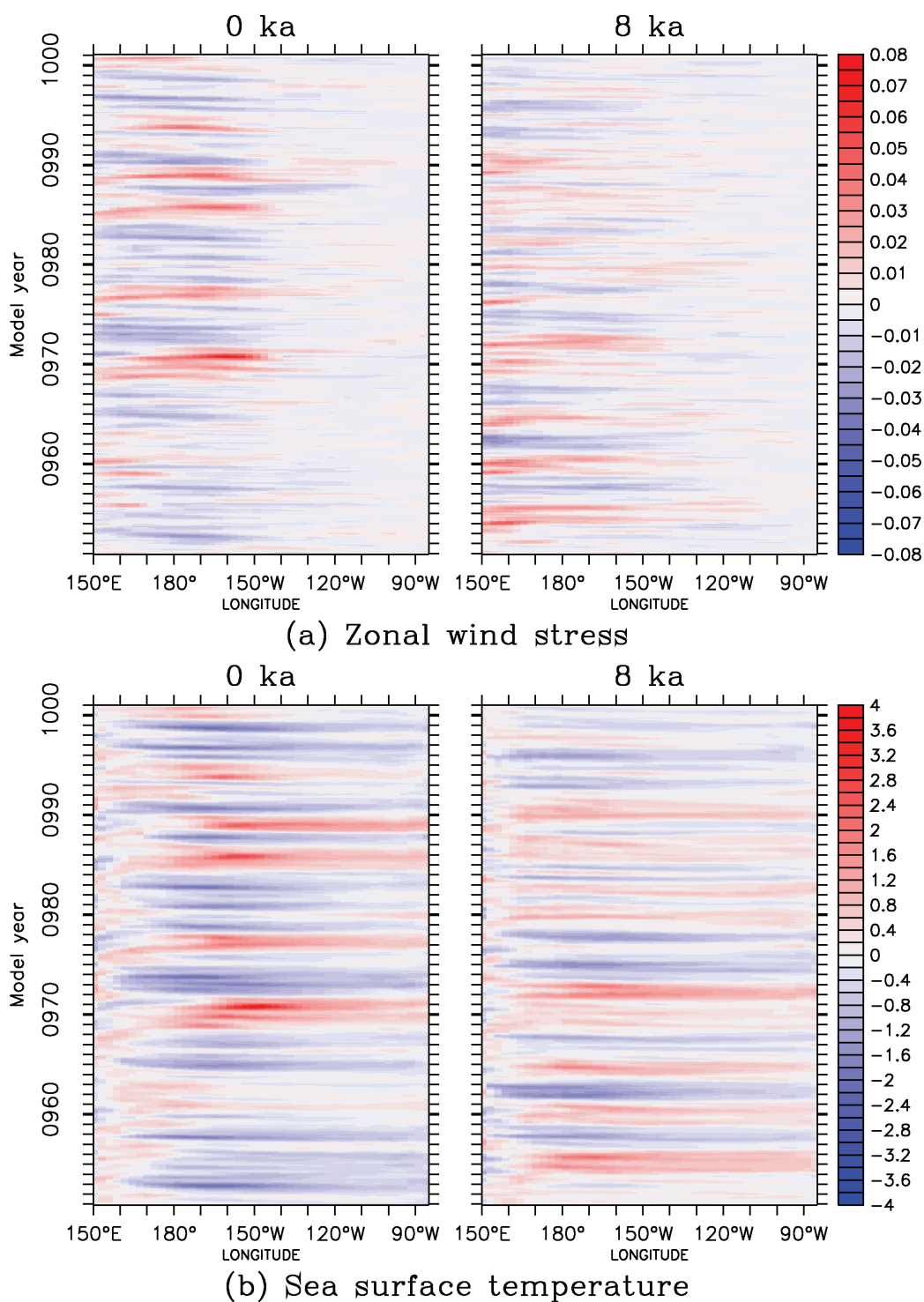
(a) Zonal wind stress

(b) Sea surface temperature

Figure 3. Monthly anomalies at the equator, relative to the mean seasonal cycle, for the final 50 years of the 0 ka and 8 ka simulations: (a) zonal wind stress (Nm^{-2}), and (b) sea surface temperature (K). The values shown are the five-month running mean.

for the simulated peak at 1 ka. Other mechanisms may therefore be at work.

Future studies should examine the changes in the magnitude, frequency and duration characteristics of El Niño events, and should investigate the effects of the changes in the atmospheric circulation upon ENSO modes. The current study only considers the role of the Earth's orbital geometry in driving changes in ENSO behaviour, and future work should therefore investigate the role of other factors, including volcanic activity and changes in solar luminosity and atmospheric greenhouse gases. The equilibrium response of CSIRO Mk3L to a doubling of the CO_2 concentration is a reduction of just 8% in the ENSO amplitude [12]. Changes in greenhouse gases may therefore have played only a minor role in the changes in ENSO behaviour over the past 8,000 years; however, this hypothesis should be thoroughly tested using multiple climate models.

4. Conclusions

By forcing a climate system model with orbitally-driven insolation changes, we have been able to reproduce the trends in ENSO variability over the past 8,000 years. Decreasing summer insolation over this period has resulted in a weakening of the Asian summer monsoon. This has reduced the stability of the background state of the tropical Pacific, creating conditions more favourable for El Niño development. However, other mechanisms may also be at work. A full understanding of the processes that drive changes in ENSO variability may be within grasp, but will require an approach that integrates the data, modelling and theory communities.

References

[1] Philander S G 1990 *El Niño, La Niña, and the Southern Oscillation* (Academic Press)

[2] Rodbell D T, Seltzer G O, Anderson D M, Abbott M B, Enfield D B and Newman J H 1999 *Science* **283** 516–520

[3] Tudhope A W, Chilcott C P, McCulloch M J, Cook E R, Chappell J, Ellam R M, Lea D W, Lough J M and Shimmield G B 2001 *Science* **291** 1511–1517

[4] Moy C M, Seltzer G O, Rodbell D T and Anderson D M 2002 *Nature* **420** 162–165

[5] McGregor H V and Gagan M K 2004 *Geophysical Research Letters* **31** L11204

[6] Monnin E, Steig E J, Siegenthaler U, Kawamura K, Schwander J, Stauffer B, Stocker T F, Morse D L, Barnola J M, Bellier B, Raynaud D and Fischer H 2004 *Earth and Planetary Science Letters* **224** 45–54

[7] Liu Z, Kutzbach J and Wu L 2000 *Geophysical Research Letters* **27** 2265–2268

[8] Clement A C, Seager R and Cane M A 2000 *Paleoceanography* **15** 731–737

[9] Zheng W, Braconnot P, Guilyardi E, Merkel U and Yu Y 2008 *Climate Dynamics* **30** 745–762

[10] Phipps S J 2006 The CSIRO Mk3L climate system model Tech. Rep. 3 Antarctic Climate and Ecosystems Cooperative Research Centre Hobart, Tasmania, Australia

[11] Brown J, Collins M, Tudhope A W and Toniazzo T 2008 *Climate Dynamics* **30** 19–36

[12] Phipps S J *in preparation*